ChemComm

COMMUNICATION

View Article Online
View Journal | View Issue

A carbon nanotube/quantum dot based photoelectrochemical biosensing platform for the direct detection of microRNAs†

Huijuan Cao, Shanshan Liu, Wenwen Tu,* Jianchun Bao and Zhihui Dai*

Cite this: *Chem. Commun.*, 2014, **50**, 13315

Received 8th August 2014,
Accepted 9th September 2014

DOI: 10.1039/c4cc06214k

www.rsc.org/chemcomm

A versatile photoelectrochemical biosensing platform was developed based on DNA–CdS quantum dots (QDs) sensitized single-walled carbon nanotubes (SWCNTs)-COOH. Combining with cyclic enzymatic amplification, a convenient, sensitive and specific biosensor for the direct detection of microRNAs (miRNAs) was designed, which provided a novel approach for analysis of miRNAs.

Photoelectrochemical measurements are a newly developed analytical technique for biological assays and have received considerable attention in recent years.[1] Due to the complete separation of the excitation source (light) and the detection signal (current), the background signal in photoelectrochemical techniques is reduced, and the detection sensitivity improves significantly.[2] Furthermore, photoelectrochemical measurements are more rapid, convenient, and sensitive and have greater accuracy than conventional optical and electrochemical methods.[3] Given these desirable advantages, much effort has been devoted toward the photoelectrochemical detection of DNA, cells, proteins, and some small molecules.[3,4] Among the numerous photoelectrochemically active species, CdS QDs have appeared as preeminent materials for photoelectrochemical analysis[4c,5] due to their stability against photobleaching, chemical stability and biocompatibility. Thus, a number of biomolecule-labeled CdS QDs, such as DNA-labeled CdS QDs, have been applied to biological analysis. However, traditionally, DNA-labeled CdS QDs have been prepared by linking pre-synthesized CdS QDs to DNA using coupling reactions or covalent binding.[6] The use of pre-synthesized QDs is time-consuming and unfavorable for simplifying operations,[7a] thus limiting its applications in photoelectrochemical measurements. Therefore, one-step synthesis of DNA-labeled QDs, which is convenient,[7] substituted the pre-synthesized method in this work. The approach relied on the design of oligonucleotides that contained two different domains: one that phosphorothioates (ps)-DNA (ps: sulphur-containing variants of the phosphodiester backbone) would be liganded to the CdS QDs, and one that phosphates (po)-DNA would be capable of molecular recognition.[7] Although po-DNA could interact with CdS,[8] Cd^{2+} was known to exhibit a 3000-fold preference for sulphur over oxygen binding when presented with nucleotides. Thus Cd^{2+} would give preference to interact with ps-DNA,[7b] and then it formed the structure of DNA-CdS QDs as shown in Scheme 1. Because of their high electrical and thermal conductivities, high surface areas, and good stability in solar cells,[9] single-walled carbon nanotubes (SWCNTs) were introduced to enhance the photocurrent and further improved the sensitivity for photoelectrochemical biosensing.

MicroRNAs (miRNAs) are a class of small endogenous non-coding RNAs (typically 19–23 nucleotides in length)[10] that play significant regulatory roles in a variety of biological processes.[10b,11] In particular, miRNAs have been functioning as diagnostic biomarkers for cancer classification, diagnosis and prognosis.[12] Therefore, various methodologies have been proposed to detect miRNAs, including northern blots, microarrays, real-time reverse transcription polymerase chain reactions, and nanoparticle-based signal amplification detection methods.[13] Electrophoretic, fluorescent, electrochemical and colorimetric[14] techniques have also been developed for the

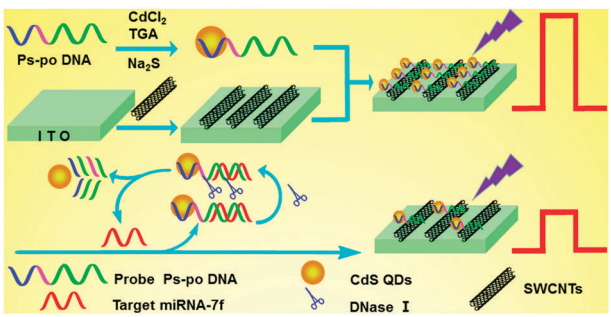

Scheme 1 Schematic illustration of the photoelectrochemical biosensor for microRNA detection.

Jiangsu Collaborative Innovation Center of Biomedical Functional Materials and Jiangsu key Laboratory of Biofunctional Materials, College of Chemistry and Materials Science, Nanjing Normal University, Nanjing, 210023, P. R. China. E-mail: daizhihuii@ninu.edu.cn, wwt@njnu.edu.cn; Fax: +86-25-85891051; Tel: +86-25-85891051

† Electronic supplementary information (ESI) available: Experimental details, characterization, photoelectrochemical response, and optimization conditions. See DOI: 10.1039/c4cc06214k

analysis of miRNAs. Although these techniques had adequate sensitivity, they suffered from the need for expensive equipment and reagents, are time-consuming, and required harsh conditions, such as high potentials. Thus, the development of new methods for the detection of miRNAs at low potentials that are rapid, convenient, sensitive, selective and quantitative is urgently required. The photoelectrochemical techniques described here could satisfy these requirements.

In this work, a versatile photoelectrochemical biosensing platform was developed based on DNA-CdS QD-sensitized SWCNTs-COOH. One-pot synthesized DNA-CdS QDs were combined with SWCNTs-COOH through π–π stacking to form DNA-labeled CdS QDs-sensitized SWCNTs-COOH as the photoelectrochemically active species. These constructions exhibited high photovoltaic conversion efficiency and good stability. Using miRNA-7f as a model, which made a large quantity of CdS QDs break away from SWCNTs-COOH after hybridizing with DNA probes[15] to decline the photocurrent, a novel signal-off photoelectrochemical biosensor was constructed (Scheme 1). In the absence of target miRNAs, a higher photocurrent could be detected due to the π–π stacking interactions between the single-stranded (ss) DNA and the SWCNTs-COOH. Specifically, this strategy was designed to enable the direct detection of miRNAs as an alternative to the standard indirect method for detection of miRNAs. In addition, this approach used a less complex procedure. Moreover, DNase I was adopted in this work to further amplify the signal. DNase I is an endonuclease that nonspecifically cleaves the DNA in RNA–DNA complexes but does not cleave RNA.[16] SsDNA-labeled CdS QDs were promptly adsorbed onto SWCNTs-COOH *via* π–π stacking interactions which prevented DNase I from approaching the constrained ssDNA and made CdS QDs adsorb firmly on SWCNTs-COOH,[16] leading to produce an intense photocurrent. However, when hybridized with miRNA, the ssDNA/miRNA bound weakly to SWCNTs-COOH, and then CdS QDs as photoelectrochemically active species would break away from SWCNTs-COOH and release into the solution where the DNA probe could be immediately hydrolyzed by DNase I while the miRNA remained intact,[16] thereby achieving photocurrent signal amplification (Scheme 1). In the work reported here, a novel, sensitive and selective method for the direct detection of miRNAs using visible light irradiation at a low potential was developed, which may find applications in other related biological assays.

To demonstrate that CdS QDs were combined with DNA, UV-Vis absorption spectra were obtained (Fig. 1A). DNA had a typical absorption peak at 260 nm (curve a). The broad absorption peaks of CdS QDs (curve b) and DNA-CdS QDs (curve c) were observed at approximately 370 nm. Compared with the UV-Vis absorption spectra of CdS QDs, the absorption band of DNA-CdS QDs (from 272 to 302 nm) was bathochromically shifted, which implied that DNA was bound to the CdS QDs.[7a]

The HRTEM images depicted the formation of CdS QDs (Fig. S1A in the ESI†) and SWCNTs-COOH (Fig. S1B in ESI†). The diameter of CdS QDs ranged from 4 to 9 nm. A highly dense deposit of DNA-CdS QDs on SWCNTs-COOH formed *via* π–π stacking interactions between SWCNTs and DNA could be observed (Fig. S1C in the ESI†), which was beneficial for photoinduced electron transfer between CdS QDs and SWCNTs-COOH.

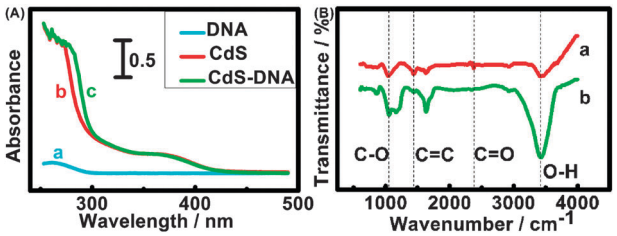

Fig. 1 (A) UV-Vis absorption spectra of DNA (a), CdS QDs (b) and DNA-CdS QDs (c). (B) FTIR spectra of pristine SWCNTs (a) and SWCNTs-COOH (b).

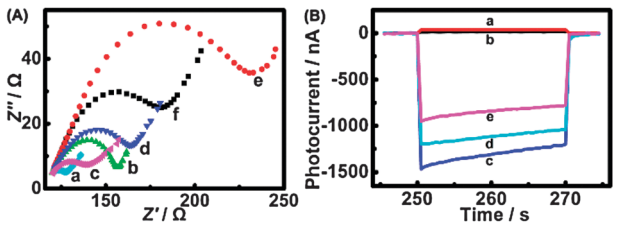

Fig. 2 (A) Nyquist diagrams of bare ITO (a), ITO/APTES (b), ITO/APTES/SWCNTs-COOH (c), ITO/APTES/SWCNTs-COOH/probe DNA (d), ITO/APTES/SWCNTs-COOH/probe DNA/Tween 20 (e), and ITO/APTES/SWCNTs-COOH/probe DNA/Tween 20/miRNA-7f (100 pM) (f). (B) The photoelectrochemical responses of ITO/DNA-CdS (a), ITO/SWCNTs-COOH (b), ITO/SWCNT-COOH/DNA-CdS (c), ITO/SWCNTs-COOH/DNA-CdS/Tween 20 (d), and ITO/SWCNTs-COOH/DNA-CdS/Tween20/miRNA-7f (10 pM) (e).

The FTIR spectra of the pristine SWCNTs and SWCNTs-COOH are shown in Fig. 1B. The C=C and C–O stretching vibrations of the pristine SWCNTs were observed at 1438 and 1043 cm^{-1}, respectively (curve a). The C=O and O–H stretching vibrations of SWCNTs-COOH were observed at approximately 1622 and 3427 cm^{-1}, respectively (curve b). Compared with the FTIR spectra of the pristine SWCNTs, the intensities of the carboxyl groups obviously increased in the FTIR spectrum of SWCNTs-COOH, indicating that hydrophilic carboxylate groups were introduced onto SWCNT surfaces.

Electrochemical impedance spectra (EIS) were used to investigate the fabrication of the photoelectrochemical biosensor (Fig. 2A). The EIS includes a semicircle portion and a linear portion. The semicircle diameter is equal to the electron-transfer resistance (R_{et}). The bare ITO electrode exhibited the lowest R_{et} (curve a). After modification with APTES (curve b), the R_{et} clearly increased, which may be attributed to the APTES film hindering the access of the redox probe ($[Fe(CN)_6]^{3-}/[Fe(CN)_6]^{4-}$) to the electrode surface. Subsequently, SWCNTs-COOH were covalently bonded to the ITO/APTES films *via* reactions between the amine and carboxyl groups, displaying a low R_{et} (curve c). This suggested that SWCNTs-COOH accelerated electron transfer between the redox probe and the electrode surface due to their excellent electronic conductivity. Then, probe DNA was introduced to the electrode surface *via* π–π stacking between ssDNA and SWCNTs-COOH, and R_{et} increased (curve d), primarily due to the negative charges of the DNA phosphate backbone, which repelled the transfer of the negatively charged probe ($[Fe(CN)_6]^{3-/4-}$). The increase of R_{et} verified the successful assembly of the probe DNA on the electrode surface. After blocking

with Tween 20 (curve e), R_{et} increased further, owing to a steric hindrance effect that impeded electron transfer between the redox probe and the electrode surface. However, after the introduction of the target RNA (curve f), R_{et} decreased dramatically compared with that of curve e. This phenomenon indicated the successful hybridization of the target RNA with the probe DNA. The changes in electron transfer resistance verified the successful fabrication of the photoelectrochemical biosensor.

The photocurrent responses following each modification step under 405 nm irradiation at an applied potential of −0.05 V are shown in Fig. 2B. When DNA-CdS was assembled on an APTES-modified ITO electrode, an anodic photocurrent of 40 nA was observed (curve a). When SWCNTs-COOH were deposited on an APTES-modified ITO electrode, an anodic photocurrent of 20 nA was generated (curve b). However, it was interesting to note that the CdS QD-sensitized SWCNT-COOH-modified ITO electrode exhibited a significantly enhanced cathodic photocurrent of 1.20 μA (curve c), which was 30- and 60-fold higher than the photocurrent observed with DNA-CdS (curve a) and SWCNTs-COOH (curve b) modified ITO electrodes, respectively. The dramatically improved photocurrent achieved with the CdS QD-sensitized SWCNT-COOH-modified ITO electrode could be attributed to two possible causes. Firstly, SWCNTs-COOH were efficient acceptors that enhanced photoinduced electron transport and prevented the charge recombination of excited CdS[9c] owing to their unique one-dimensional nanostructure and appropriate band energy. Secondly, ssDNA can interact with SWCNTs-COOH *via* π–π stacking. Thus, CdS QDs were linked to the SWCNTs-COOH, leading to a significantly improved photocurrent response. After the electrode was treated with Tween 20 to block nonspecific adsorption, the photocurrent declined (curve d), which was most likely due to an enhanced steric hindrance effect that blocked the diffusion of the electron donors to the surfaces of the photoelectrochemically active material. However, a dramatically decreased photocurrent of 495 nA was observed after hybridization with probe miRNA-7f (curve e), which was only 41% of the photocurrent with the CdS QDs-sensitized SWCNTs-COOH-modified ITO electrodes (curve c). After DNA probe hybridization with miRNA-7f, a large amount of DNA-CdS separated from the SWCNTs-COOH due to their weak non-covalent interactions. The large quantity of CdS QDs that broke away from the SWCNTs-COOH resulted in a greatly declined photocurrent, leading to the above phenomenon (Scheme 1).

Upon irradiation with light, electrons were excited from the valence band (VB) and then transferred to the conduction band (CB) of CdS QDs, thus yielding electron–hole pairs.[1] At a negatively applied bias (−0.05 V), protons (H^+) in the PBS captured the partial photoinduced electrons from the CB electrons of CdS QDs, producing H_2.[17] Ascorbic acid (AA) was chosen as a nontoxic electron donor to scavenge the VB holes. Finally, the residual photoinduced electrons were collected by SWCNTs-COOH. SWCNTs-COOH served as good photoelectron acceptors and improved the activity of CdS QDs due to their excellent capacity for photoinduced electron transport. SWCNTs-COOH also inhibited the charge recombination of the electron–hole pairs of the excited CdS QDs, generating a stable cathodic photocurrent and enhancing the overall photovoltaic conversion efficiency. Moreover, the photocurrent could be turned on and off by controlling the light (Fig. S2 in the ESI†). Based on the high photovoltaic conversion efficiency and good stability of the SWCNTs-COOH/DNA-CdS/Tween 20 films, they were used advantageously to develop a photoelectrochemical detection platform under visible light irradiation at low potentials.

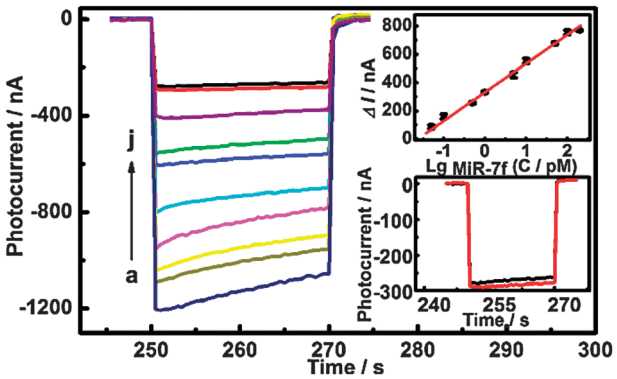

Fig. 3 Photoelectrochemical responses of the biosensor to a blank (a) and to 50 fM, 100 fM, 500 fM, 1 pM, 5 pM, 10 pM, 50 pM, 100 pM, and 200 pM miRNA-7f (b–j, respectively). Upper inset: linear calibration; lower inset: magnified responses of (i) and (j).

Under optimized conditions (Fig. S3 in the ESI†), the photoelectrochemical biosensor was applied to the detection of miRNA-7f at different concentrations (from 0 to 200 pM). The photocurrent responses obtained by varying the miRNA-7f concentrations (C) are shown in Fig. 3. The photocurrents decreased with increasing concentrations of miRNA-7f. The calibration curve was established by plotting ΔI ($\Delta I = I - I_0$, where I is the photocurrent of the miRNA-7f solution at a particular concentration, and I_0 is the background photocurrent) against the miRNA-7f concentration in the linear range from 50 fM to 100 pM. The calibration equation was $I = 331.4 + 203.3\lg C$, with a correlation coefficient R of 0.9953, where I is the photocurrent and C is the concentration of miRNA-7f. The detection limit was estimated to be 34 fM at a signal-to-noise ratio of 3. The linear range was much wider and the detection limit was lower than those reported in previous work[16,18] (Table S1 in the ESI†). Therefore, the photoelectrochemical biosensor exhibited a wide linear response range, and high sensitivity and selectivity in the determination of miRNA at low potentials.

To evaluate the selectivity of the proposed method, three representative members of the let-7 family were investigated, including the complementary target (let-7f: 5′-UGA GGU AGU AGA UUG UAU AGUU-3′), a single-base mismatched strand (let-7a: 5′-UGA GGU AGU AGG UUG UAU AGUU-3′) and a three-base mismatched strand (let-7d: 5′-AGA GGU AGU AGG UUG CAU AGUU-3′), under the same conditions. As shown in Fig. 4, the photocurrent response to let-7f (column a) was approximately 2.41-fold greater than that to let-7a (column b). In addition, the response to let-7d (column c) was 14.02% of that of let-7f. This level of mismatch discrimination ability was better than that of other previous miRNA hybridization-based biosensors.[19] Thus, the proposed photoelectrochemical biosensor had high selectivity for detection of miRNAs.

In summary, a versatile photoelectrochemical biosensing platform was developed based on CdS QD-sensitized SWCNTs-COOH. A highly dense deposit of DNA-CdS QDs on SWCNTs-COOH was beneficial for photoinduced electron transfer between CdS QDs

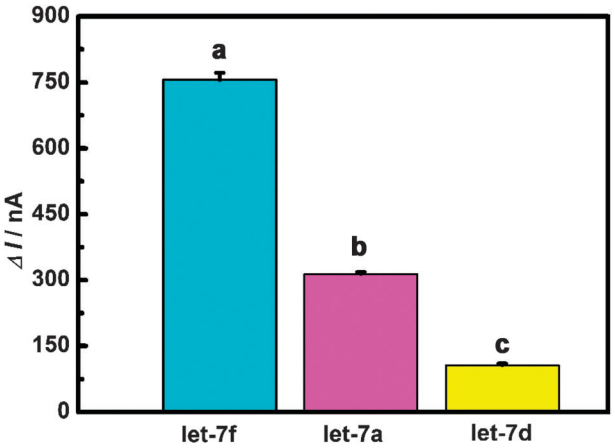

Fig. 4 Photocurrent changes in the photoelectrochemical biosensor towards miRNA-7f (100 pM) (a), miRNA-7a (100 pM) (b) and miRNA-7d (100 pM) (c).

and SWCNTs-COOH. SWCNTs-COOH served as a good photoelectron acceptor and enhanced the photoinduced electron transport while inhibiting charge recombination of the electron–hole pairs in the excited CdS QDs, hence generating a cathodic photocurrent. Using miRNA-7f as a model, a novel signal-off photoelectrochemical biosensor for the direct detection of miRNA was constructed. MiRNA-7f caused a large quantity of CdS QDs to break away from the SWCNTs-COOH after hybridizing with a target DNA probe, resulting in a decrease in the photocurrent. Combined with cyclic enzymatic amplification, the photoelectrochemical biosensor exhibited good analytical performance for the detection of miRNA-7f. Because different probes can specifically bind to different miRNAs, the designed strategy has an expansive perspective of applications to detection of other miRNAs and for the construction of versatile photoelectrochemical platforms. Nevertheless, realizing simultaneously multiplex miRNAs analysis in real samples will be the biggest challenge.

This work was supported by the National Natural Science Foundation of China for the project (21475062, 21175069 and 21205061), Natural Science Foundation of Jiangsu (BK2012448), Research Fund for the Doctoral Program of Higher Education of China (20113207110005 and 20123207120007) and Foundation of the Jiangsu Education Committee (11KJA150003 and 12KJB150016). We appreciate the financial support from the Priority Academic Program Development of Jiangsu Higher Education Institutions.

Notes and references

1 W. W. Zhao, J. Wang, J. J. Xu and H. Y. Chen, *Chem. Commun.*, 2011, **47**, 10990.
2 X. R. Zhang, S. G. Li, X. Jin and S. S. Zhang, *Chem. Commun.*, 2011, **47**, 4929.
3 W. W. Zhao, Z. Y. Ma, P. P. Yu, X. Y. Dong, J. J. Xu and H. Y. Chen, *Anal. Chem.*, 2012, **84**, 917.
4 (*a*) Y. R. An, L. L. Tang, X. L. Jiang, H. Chen, M. C Yang, L. T. Jin, S. P. Zhang, C. G. Wang and W. Zhang, *Chem. – Eur. J.*, 2010, **16**, 14439; (*b*) Y. P. Wu, B. T. Zhang and L. H. Guo, *Anal. Chem.*, 2013, **85**, 6908; (*c*) X. M. Zhao, S. W. Zhou, L. P. Jiang, W. H. Hou, Q. M. Shen and J. J. Zhu, *Chem. – Eur. J.*, 2012, **18**, 4974; (*d*) E. Golub, A. Niazov, R. Freeman, M. Zatsepin and I. Willner, *J. Phys. Chem. C*, 2012, **116**, 13827.
5 (*a*) G. L. Wang, P. P. Yu, J. J. Xu and H. Y. Chen, *J. Phys. Chem. C*, 2009, **113**, 11142; (*b*) F. X. Xiao, J. W. Miao and B. Liu, *J. Am. Chem. Soc.*, 2014, **136**, 1559; (*c*) D. R. Baker and P. V. Kamat, *Adv. Funct. Mater.*, 2009, **19**, 805.
6 (*a*) M. S. Wu, H. W. Shi, J. J. Xu and H. Y. Chen, *Chem. Commun.*, 2011, **47**, 7752; (*b*) Y. Cheng, Y. Huang, J. P. Lei, L. Zhang and H. X. Ju, *Anal. Chem.*, 2014, **86**, 5158.
7 (*a*) C. L. Zhang, J. Xu, S. M. Zhang, X. H. Ji and Z. K. He, *Chem. – Eur. J.*, 2012, **18**, 8296; (*b*) G. Tikhomirov, S. Hoogland, P. E. Lee, A. Fischer, E. H. Sargent and S. O. Kelley, *Nat. Nanotechnol.*, 2011, **6**, 485; (*c*) N. Ma, E. H. Sargent and S. O. Kelley, *Nat. Nanotechnol.*, 2009, **4**, 121.
8 C. W. Ge, M. Xu, J. H. Fang, J. P. Lei and H. X. Ju, *J. Phys. Chem. C*, 2008, **112**, 10602.
9 (*a*) C. Oelsner, M. A. Herrero, C. Ehli, M. Prato and D. M. Guldi, *J. Am. Chem. Soc.*, 2011, **133**, 18696; (*b*) A. Kongkanand and P. V. Kamat, *ACS Nano*, 2007, **1**, 13; (*c*) B. Farrow and P. V. Kamat, *J. Am. Chem. Soc.*, 2009, **131**, 11124.
10 (*a*) D. P. Bartel, *Cell*, 2004, **116**, 281; (*b*) L. He and G. J. Hannon, *Nat. Rev. Genet.*, 2004, **5**, 522; (*c*) S. Griffiths-Jones, H. K. Saini, S. V. Dongen and A. J. Enright, *Nucleic Acids Res.*, 2008, **36**, 154.
11 (*a*) M. S. Nicoloso, R. Spizzo, M. Shimizu, S. Rossi and G. A. Calin, *Nat. Rev. Cancer*, 2009, **9**, 293; (*b*) B. R. Cullen, *Nature*, 2009, **457**, 421; (*c*) V. Ambros, *Cell*, 2003, **113**, 673; (*d*) S. S. Hebert and B. D. Strooper, *Science*, 2007, **317**, 1179; (*e*) A. Esquela-Kerscher and F. J. Slack, *Nat. Rev. Cancer*, 2006, **6**, 259.
12 (*a*) A. W. Wark, H. J. Lee and R. M. Corn, *Angew. Chem., Int. Ed.*, 2008, **47**, 644; (*b*) H. F. Dong, J. P. Lei, H. X. Ju, F. Zhi, H. Wang, W. J. Guo, Z. Zhu and F. Yan, *Angew. Chem., Int. Ed.*, 2012, **51**, 4607; (*c*) L. He, J. M. Thomson, M. T. Hemann, E. Hernando-Monge, D. Mu, S. Goodson, S. Powers, C. Cordon-Cardo, S. W. Lowe, G. J. Hannon and S. M. Hammond, *Nature*, 2005, **435**, 828.
13 (*a*) G. S. Pall and A. J. Hamilton, *Nat. Protoc.*, 2008, **3**, 1077; (*b*) P. T. Nelson, D. A. Baldwin, L. M. Scearce, J. C. Oberholtzer, J. W. Tobias and Z. Mourelatos, *Nat. Methods*, 2004, **1**, 1; (*c*) N. Redshaw, T. Wilkes, A. Whale, S. Cowen, J. Huggett and C. A. Foy, *Biotechniques*, 2013, **54**, 155; (*d*) E. Crew, S. Rahman, A. Razzak-Jaffar, D. Mott, M. Kamundi, G. Yu, N. Tchah, J. Lee, M. Bellavia and C. J. Zhong, *Anal. Chem.*, 2012, **84**, 26.
14 (*a*) B. J. Dodgson, A. Mazouchi, D. W. Wegman, C. C. Gradinaru and S. N. Krylov, *Anal. Chem.*, 2012, **84**, 5470; (*b*) T. Tian, H. Xiao, X. L. Zhang, S. A. Peng, X. E. Zhang, S. Guo, S. R. Wang, S. M. Liu, X. Zhou, C. Meyers and X. Zhou, *Chem. Commun.*, 2013, **49**, 75; (*c*) Z. L. Ge, M. H. Lin, P. Wang, H. Pei, J. Yan, J. Y. Shi, Q. Huang, D. N. He, C. H. Fan and X. L. Zuo, *Anal. Chem.*, 2014, **86**, 2124; (*d*) J. Park and J. S. Yeo, *Chem. Commun.*, 2014, **50**, 1366.
15 M. Wu, R. Kempaiah, P. J. Huang, V. Maheshwari and J. W. Liu, *Langmuir*, 2011, **27**, 2731.
16 L. Cui, X. Y. Lin, N. H. Lin, Y. L. Song, Z. Zhu, X. Chen and C. J. Yang, *Chem. Commun.*, 2012, **48**, 194.
17 Q. Li, B. D. Guo, J. G. Yu, J. R. Ran, B. H. Zhang, H. J. Yan and J. R. Gong, *J. Am. Chem. Soc.*, 2011, **133**, 10878.
18 (*a*) H. S. Yin, Y. L. Zhou, H. X. Zhang, X. M. Meng and S. Y. Ai, *Biosens. Bioelectron.*, 2012, **33**, 247; (*b*) Z. Gao and Y. H. Yu, *Biosens. Bioelectron.*, 2007, **22**, 933; (*c*) Y. Zhang, Z. Li, Y. Cheng and X. Lv, *Chem. Commun.*, 2009, 3172; (*d*) Q. Xi, D. M. Zhou, Y. Y. Kan, J. Ge, Z. K. Wu, R. Q. Yu and J. H. Jiang, *Anal. Chem.*, 2014, **86**, 1361.
19 Y. Q. Wen, Y. Xu, X. H. Mao, Y. L. Wei, H. Y. Song, N. Chen, Q. Huang, C. H. Fan and D. Li, *Anal. Chem.*, 2012, **84**, 7664.

